

## AN INNER RING AND THE MICRO LENSING TOWARD THE BULGE

MAARTJE N. SEVENSTER<sup>1</sup> AND AGRIS J. KALNAJS<sup>2</sup>  
 MSSSO/RSAA, Cotter Road, Weston ACT 2611, Australia

*Draft version November 25, 2018*

### ABSTRACT

All current Bulge–Disk models for the inner Galaxy fall short of reproducing self–consistently the observed micro–lensing optical depth by a factor of two ( $> 2\sigma$ ). We show that the least mass–consuming way to increase the micro–lensing optical depth is to add density roughly half–way the observer and the highest micro–lensing–source density. We present evidence for the existence of such a density structure in the Galaxy: an inner ring, a standard feature of barred galaxies. Judging from data on similar rings in external galaxies, an inner ring can contribute more than 50% of a pure Bulge–Disk model to the micro–lensing optical depth. We may thus eliminate the need for a small viewing angle of the Bar. The influence of an inner ring on the event–duration distribution, for realistic viewing angles, would be to increase the fraction of long–duration events toward Baade’s window. The longest events are expected toward the negative–longitude tangent point at  $\ell \sim -22^\circ$ . A properly sampled event–duration distribution toward this tangent point would provide essential information about viewing angle and elongation of the over–all density distribution in the inner Galaxy.

*Subject headings:* Galaxy: structure – ISM: structure

### 1. INTRODUCTION

The “micro–lensing optical depth” as a function of position on the sky is the probability that a given star in that direction will be gravitationally lensed by a foreground object at a given instant. The micro–lensing optical depth  $\tau$  measured toward the Bulge (or Baade’s window) (the MACHO project, Alcock et al. 1997; the OGLE project, Udalski et al. 1994; the DUO project, Alard & Guilbert 1997) provides important information about the stellar and dark–matter distribution in the inner Galaxy.

Other than for the Magellanic Clouds, one usually tries to explain the Bulge’s micro–lensing optical depth with “self–lensing” models; the lenses and the sources come from the same (dynamical) distribution. Justification for this comes from the micro–lensing event–duration distribution, as well as recent determinations of the initial–mass function and the fraction of invisible matter in the solar neighbourhood, all of which indicate that there is no significant amount of dark matter in the plane of the Galaxy nor a large number of brown dwarfs (Alcock et al. 1997; Gould, Flynn & Bahcall 1998; Kroupa 1998; Kuijken & Gilmore 1989; Fuchs, Jahreiss & Flynn 1998). Note that even for the lines of sight toward the LMC, in fact, dark matter plays a minor role in microlensing (Alcock et al. 2000b).

The high measured value of  $\tau$  by Alcock et al. (1997) could be reproduced by a barred density distribution, if oriented almost parallel to the line of sight (Zhao & Mao 1996). However, this is not within the scope of realistic models that reproduce observed stellar surface densities and kinematics (Binney, Gerhard & Spergel 1997; Bisantz et al. 1997; Zhao, Rich & Spergel 1996; Nikolaev & Weinberg 1997; Fux 1997; Sevenster et al. 1999). A larger scaleheight of the Bar and/or the Disk component,  $\sim 400$ pc, or scale of the inner Halo (see Minniti 1996) could

also increase the micro–lensing optical depth, but cannot be reconciled with the rapid decline of micro–lensing optical depth with latitude (Alcock et al. 1997). Hence, a large apparent scaleheight is not an option (see also Sevenster et al. 1999). To the best of our present knowledge, the distribution of stars in the exponential Disk and the Bar or the Bulge does not account for the observed micro–lensing optical depth, given the limits on the mass–to–light ratio.

In this paper, we will try to resolve this controversy. Throughout this article, we will adopt  $R_\odot \equiv 8$  kpc, unless it is used as a generic symbol of distance between an observer and the centre of a generic galaxy.

### 2. HOW TO ENHANCE MICRO LENSING ?

The micro–lensing optical depth  $\tau$  in a given direction depends on the distance to the lenses,  $S_1$ , and the sources,  $S_s$ , via the term  $S_1(S_s - S_1)/S_s$  (see Kiraga & Paczynski 1994). This is maximized, for one source–lens pair, if  $S_1 = 0.5S_s$ . To increase the micro–lensing optical depth one would clearly like to add density roughly between the observer and the highest density of sources: the central galactic–bulge region. Let’s define the contribution of the density at a distance  $S_1$  to the micro–lensing optical depth towards one source on the minor axis of the Galaxy, at  $S_s \equiv R_\odot$  (the latitude of the source has to be  $< 8^\circ$  so that  $\cos(b) > 0.99$ ), as

$$\begin{aligned} \Delta\tau(R, z) &= \rho(R, z) \frac{S_1(R_\odot - S_1)}{R_\odot} \Delta R \\ &= \rho_0(R) \exp[-S_1 \tan |b|/h_z] \frac{S_1(R_\odot - S_1)}{R_\odot} \Delta R, \quad (1) \end{aligned}$$

with  $(R, z)$  galacto–centric cylindrical coordinates and  $b$

<sup>1</sup>msevenst@mso.anu.edu.au

<sup>2</sup>agris@mso.anu.edu.au

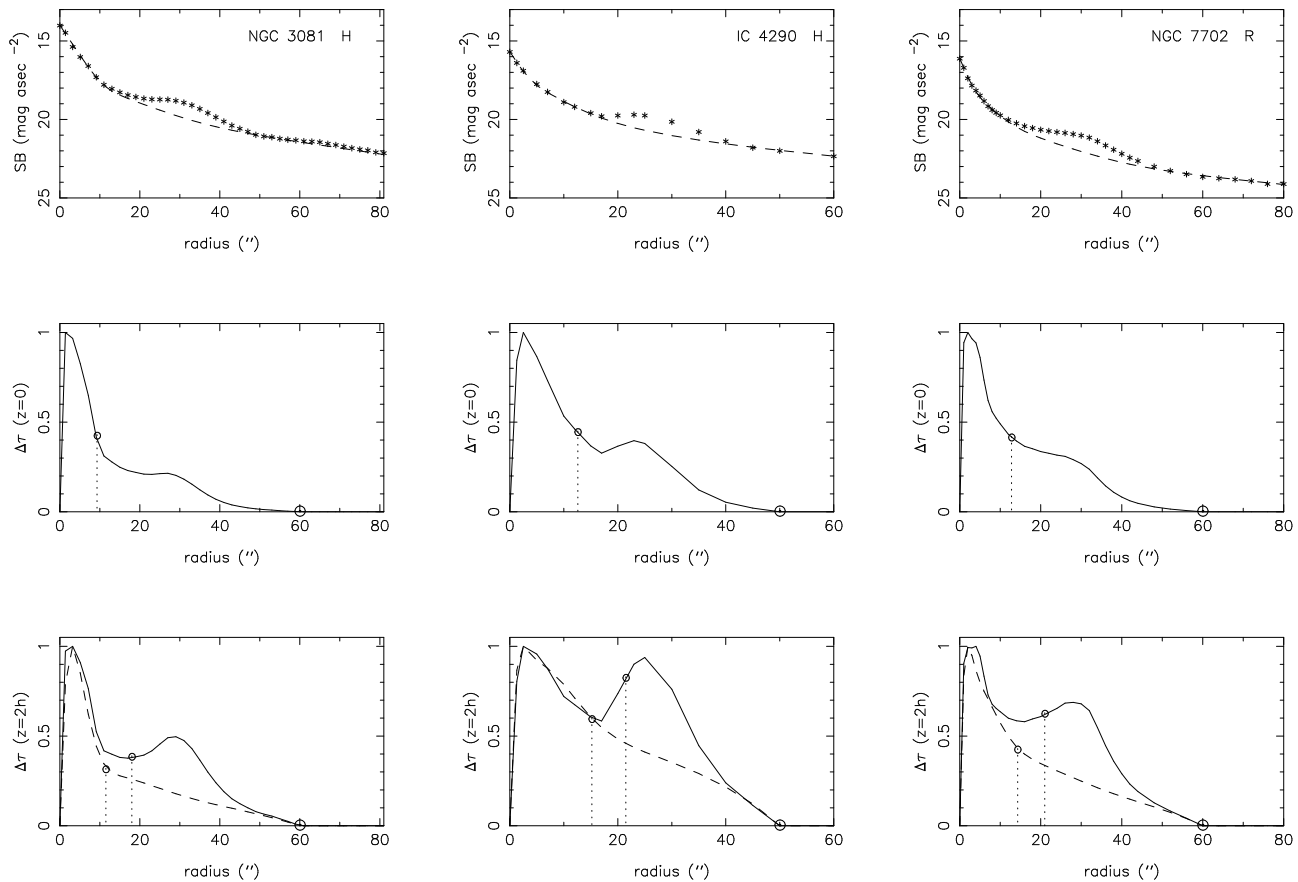


FIG. 1.— Elliptically averaged surface-density profile (dots) for the galaxy NGC 3081 (Buta & Purcell 1998), IC 4290 (Buta et al. 1998) and NGC 7702 (Buta 1991) in magnitudes per square arcsecond (top panels). The middle panels show the contribution,  $\Delta\tau$ , to the micro-lensing optical depth along the line of sight towards a source in the centre of the galaxies. The bottom panels give  $\Delta\tau$  along a line of sight slightly out of the plane (solid curves), intersecting the minor axis of the galaxy at two scaleheights (maximizing equation (3) for  $S_1=0.5 R_D$ ; see Section 2). The vertical dotted lines indicate the median radii for the line-of-sight optical depth distributions. All profiles are normalized to be 1 at maximum. For NGC 3081, the total micro-lensing optical depth (for a source at  $R=0$  and  $z=2h_z$ ) with ring is  $1.3\times$  that of only bulge and disk and the mass in the ring is 20% of the total mass. For IC 4290, the corresponding figures are  $1.4\times$  and 22%. For NGC 7702, they are  $1.5\times$  and 25%. The dashed curves in the top and bottom panels repeat the same for a three/quarter-exponential bulge-disk fit to the surface-density profiles.

galactic latitude, and the total mass involved in creating that density at that distance as

$$\Delta M(R) = 4\pi h_z R \rho_0(R) \Delta R = 4\pi h_z (R_\odot - S_1) \rho_0(R) \Delta R, \quad (2)$$

assuming the density is completely axisymmetric with constant exponential scaleheight  $h_z$ . The quantity one would like to maximize is

$$\Delta\tau/\Delta M = \frac{S_1}{4\pi h_z R_\odot} \exp[-S_1 \tan |b|/h_z], \quad (3)$$

which is maximal for  $S_1=R_\odot$  if  $b=0^\circ$  and for  $S_1=h_z/\tan |b|$  otherwise. (Beware that equation (3) only optimizes for fixed  $\tan |b|$ ; it is not a true free parameter.) In the Galaxy, with  $h_z \sim 300$  pc and the microlensing measurement at  $b \sim 4^\circ$ , this gives  $S_1=4.3$  kpc (or galacto-centric radius  $R=3.7$  kpc).

Would it be an option to have a ring of enhanced density at such a radius? In barred galaxies, one commonly observes dense rings, that trace closed orbits near resonances in the rotating potential (see Buta & Combes 1996 for a review). They contain significant mass. A so-called “inner ring”, encircling the galactic Bar, may prove an ideal candidate.

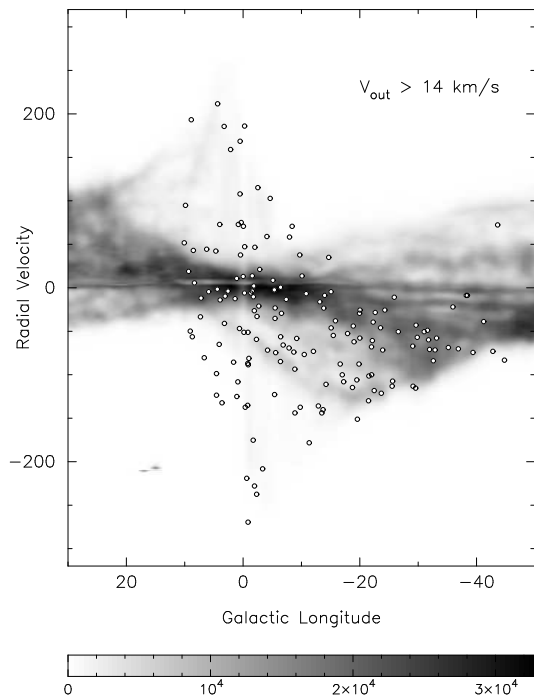


FIG. 2.— The HI longitude–velocity diagram (greyscale) for latitudes  $|b| < 1.5^\circ$ , with higher–mass OH/IR stars overplotted (circles; see Section 3). The “3–kpc arm” is the filament extending from  $(\ell, V) \sim (-20^\circ, -130 \text{ km s}^{-1})$  to  $\sim (+5^\circ, -25 \text{ km s}^{-1})$ . A suggested counterpart, the “4–kpc arm” (see Shane 1972), turns around at  $\sim (+25^\circ, 100 \text{ km s}^{-1})$ .

We demonstrate this in Fig. 1, with surface–density profiles, in the reddest available bands, and the corresponding  $\Delta\tau$  (equation 1) for three external inner–ring galaxies, NGC 3081 (SAB), IC 4290 (SB) and NGC 7702 (SA). We assume a constant, exponential scaleheight, axisymmetry and constant mass–to–light ratio across all galaxies and ignore inclination effects ( $i > 40^\circ$  for all; inclination smears

out density contrasts, but does not change the relative masses of components). The spatial density in the plane of the galaxies hence follows the surface–density profiles. We place the observer at exactly twice the ring radius in each galaxy. This optimizes equation (3) for  $\tan |b| = 2h_z/R_\odot$ , as is clear from the differences between the two lines of sight through the mass models in Fig. 1.

In all three galaxies, lensing material well in front of the bulge yields 50% of the micro–lensing optical depth toward a source situated at the centre, compared to about 30% at the same radii for the fits without ring (see Fig. 1). For the line of sight out of the plane, the rings themselves contribute 30% to 50% of the micro–lensing optical depth due to bulge and disk alone. For a lower  $\tan |b|$ , assuming smaller scaleheight while keeping the ring halfway between observer and centre of the galaxy, the relative contribution is still larger. For NGC 7702, for instance, the ring contribution is 60% when assuming a scaleheight that is half as large as used in Fig. 1.

For simplicity and clarity, in this section we calculated micro–lensing optical depth contributions with just one source on the galaxy’s minor axis. Naturally, for the full micro–lensing optical depth one needs to take into account the full distribution of sources. For source–detectability parameter  $\beta=0$  (see Section 4) and  $S_s < R_\odot$ , the rings’ relative contributions to the true micro–lensing optical depth are virtually the same as the fractions given in the caption of Fig. 1, confirming the validity of our simpler approach. For smaller distance cut–off the fraction is higher, and vice versa; for  $\beta=-1$  the fraction is lower.

### 3. AN INNER RING IN THE GALAXY

The “3–kpc arm” is a prominent large–scale feature seen in the kinematic distribution of galactic hydrogen (see Oort(1977) for early references). The HI emission can be followed over a range of longitudes, from  $\ell \sim 7^\circ$  to  $\ell \sim -20^\circ$  (Fig. 2). In front of the galactic Centre it is seen in absorption at a line–of–sight velocity of  $-53 \text{ km s}^{-1}$ . This measurement gives one of the most convincing arguments for non–circular motions in the galactic Disk. Many explanations have been proposed for the origin of the arm, ranging from an explosive event in the galactic Centre to non–circular motions forced by a rotating bar (Shane 1972; Yuan 1984; Binney et al. 1997; Englmaier & Gerhard 1999).

In most stellar samples such a longitude–velocity structure cannot be traced, for obvious reasons. However, we can identify nine OH/IR stars from a systematic sample as “3–kpc” stars (Fig. 2; see Sevenster 1999 for details). They do not only share their longitude–velocity structure with the HI filament, but also their latitudes: all are well within a degree from the plane. This is the first unambiguous evidence for a stellar–kinematic counterpart of the 3–kpc arm. The initial masses of these nine objects are  $\sim 4 M_\odot$ , corresponding to ages of  $\sim 0.2$  Gyr. Of the older OH/IR stars of the same sample, only one coincides with the 3–kpc longitude–velocity filament. The probability for a chance alignment with these properties is less than 1%.

For two of those stars (IRAS 17378–3100 and 17271–3425), distances are given in the literature: 4.9 kpc and 4.3 kpc, respectively (Lépine et al. 1995). Although these fit in perfectly with our scenario, they are derived using, amongst others,  $[K-L]$ , which may vary by

$\pm 1$  mag between stellar maximum and minimum (as for 17271–3425) resulting in a  $\pm 2$  kpc error for this source from the colour variability alone. This distance information clearly does not weaken our arguments, but neither does it strengthen them.

Had the 3-kpc arm been a density wave, the stars and the gas would be likely to have separated during 0.2 Gyr. Now, they are separating only on timescales expected from normal diffusion ( $\Delta U \sim 10 \text{ km s}^{-1}$  for ages of  $\sim 0.25$  Gyr, Wielen 1977). The ages of the stars and the  $53 \text{ km s}^{-1}$  expansion rate also rule out an explosive origin of the 3-kpc arm. They should be at a radius of 10 kpc by now, whereas the current position is about half way between the Sun and the Galactic center.

The evident explanation for this close association of the OH/IR stars and the hydrogen, that has survived for 2 galactic revolutions, is that they move along the same single filled elliptical orbit, swept up by the rotating Bar into an inner ring (Section 2). This is in agreement with independent determinations of the pattern speed (eg. Kalnajs 1991; Kalnajs 1996; Fux 1997). The negative-longitude tangent point is clearly identified at  $-22^\circ$  (Shane 1972; Hammersley et al. 1994; Sevenster 1999). On the positive-longitude side, the tangent point is likely to be around  $+25^\circ \pm 2^\circ$  (Shane 1972; Cohen et al. 1980; Hammersley et al. 1994; Blommaert, van Langevelde & Michiels 1994). Since inner rings share the major axis with the bar they encircle, as corroborated by the tangent point at a radius of 3 kpc, it is even less likely that we see the Bar nearly end-on (see Section 1). For small viewing angles, the velocity would vary much more slowly with longitude than observed.

Based on external ringed galaxies (Section 2), the 3-kpc ring should be a good candidate to reproduce the observed value of the micro-lensing optical depth, in the same fashion as the galaxies in Fig. 1. In the next sections, we will discuss some implications of this proposition, while avoiding to make absolute statements, as any choice of values of parameters for the ring or the other galactic components would make the discussion less general.

#### 4. MICROLENSING MEASUREMENTS

For a sample of 45 MACHO events, the calculated micro-lensing optical depth is  $2.11^{+0.47}_{-0.39} \times 10^{-6}$ , roughly corrected for blending, toward ( $\ell = 2^\circ 7$ ,  $b = -4^\circ 1$ ) on average (Alcock et al. 1997). A more recent measurement, using difference-image analysis (Alcock et al. 2000a), is even higher,  $2.43^{+0.39}_{-0.38} \times 10^{-6}$  toward ( $\ell = 2^\circ 68$ ,  $b = -3^\circ 35$ ). Fewer uncertain factors are involved when using red-clump-giant events only, although unfortunately the number statistics are not very favourable for that sample; Alcock et al. (1997) give  $\tau = 3.9^{+1.8}_{-1.2} \times 10^{-6}$  toward ( $\ell = 2^\circ 55$ ,  $b = -3^\circ 64$ ), but Popowski et al. (2000) give  $2.0^{+0.4}_{-0.4} \times 10^{-6}$  toward ( $\ell = 3^\circ 9$ ,  $b = -3^\circ 8$ ) from a preliminary analysis of the clump giants in the full MACHO sample, using four times more sources than in the Alcock et al. (1997) calculation.

When modelling the micro-lensing optical depth, an important parameter is the power of the source-distance dependence,  $\beta$  (see Kiraga & Paczynski 1994). In the full expression for  $\tau_\beta$  the source distance comes in as  $S_s^{2+2\beta}$ , so that for  $\beta = -1$  the number of detectable sources goes

up with  $S_s^2$ , as it should from the usual geometrical argument, and down with  $S_s^{-2}$ , as the sources get fainter. For sources with a very narrow range of luminosities and distances, such as red-clump giants that are very bright and only in the bulge,  $\beta = 0$  is more appropriate since they are all bright enough to be detected.

Importantly, the observations were not taken exactly towards the galactic Centre. This makes the case for the inner ring stronger, as we already saw in Section 2. For the latitude of the observations, the maximum of equation (3) would occur exactly half-way between the Sun and the galactic Centre for a scaleheight of 280 pc. Typical model values for the micro-lensing optical depth are  $0.9 \times 10^{-6}$  for  $\beta = -1$  and  $1.4 \times 10^{-6}$  for  $\beta = 0$  (Bissantz et al. 1997; Sevenster et al. 1999). A ring contribution of  $\sim 50\%$  of the bulge-disk contribution (Section 2) would bring models to within  $1.5\sigma$  below the Alcock et al. (1997) values and  $\beta = 0$  models right on the Popowski et al. (2000) value. For comparison, the spiral-arm model of Taylor & Cordes (1993), for example, would yield only of the order of a few per cent of the bulge-disk micro-lensing optical depth (and that is assuming the spiral-arm mass contrast is the same for stars as it is for gas).

The ring's contribution, in depending on the distance to the observer, will depend crucially on the semi-major axis as well as the viewing angle of the ring. Other factors are the radial and vertical extent of the ring, as discussed extensively in Section 2. Note that equation (3) is particularly suited to approximate the clump-giant measurement, with the sources close to the Galaxy's minor axis and detection chance  $\equiv 1$ .

## 5. EVENT-DURATION DISTRIBUTIONS

### 5.1. Models

For the remainder of this paper, we will concentrate on the expected influence of a ring of lenses between us and the galactic Centre on the event-duration distribution of microlensing events, relative to the durations of events in an underlying generic bulge-disk distribution. For this, we will need to know distances, positions and transverse velocities – in other words, almost the full six-dimensional coordinates – for sources and lenses, in the ring as well as the disk and bulge. We use an N-body simulation of the barred Galaxy by Fux (1997); model “m08t3200”, with  $R_\odot = 8$  kpc,  $V_\odot = 210 \text{ km s}^{-1}$ ,  $f_V = 1$  and adaptable  $\phi_{\text{bar}}$  (for a justification see also Sevenster et al. 1999). A random realization of the following ring model is added, assuming that all ring particles stream strictly along the ring-density contour :

$$\rho_{\text{ring}} = \rho_{0r} \exp(-(R_r - a)^4 / (2\delta_r^4)) \exp(-|z|/h_z),$$

$$\text{where } R_r^2 = x_\phi^2/q_r^2 + y_\phi^2 \text{ and}$$

$$x_\phi, y_\phi \text{ cartesian minor/major axis coordinates.} \quad (4)$$

As we argued in Section 3, the ring is a filled elliptical orbit, so the velocities of particles on the ring are derived assuming angular momentum is conserved. This is not strictly true in a non-axisymmetric potential, but a good approximation. Thus, the magnitudes of the ring velocities are found by fixing the angular momentum to give a radial velocity of to  $+53 \text{ km s}^{-1}$  at the position where the

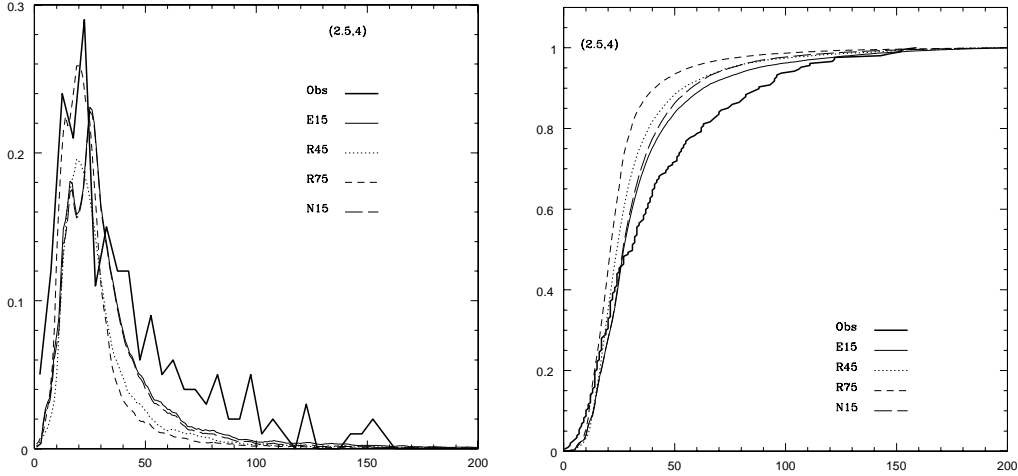


FIG. 3.— The relative (left) and cumulative relative (right) event-duration distributions ( $\beta = -1, m \equiv 1$ ) along the line of sight toward Baade's window for four different models and the MACHO observations (thick curve; 202 events from the MACHO alert webpage (1995–1999, well-determined durations < 200 days only, excluding field 301). Bootstrapping the model distributions, we find that there are no biases in the CEDDs and the errors are below 0.01 (largest around 20 days). Note that the models are not fits to the observations. The ordinate gives the event duration in days.

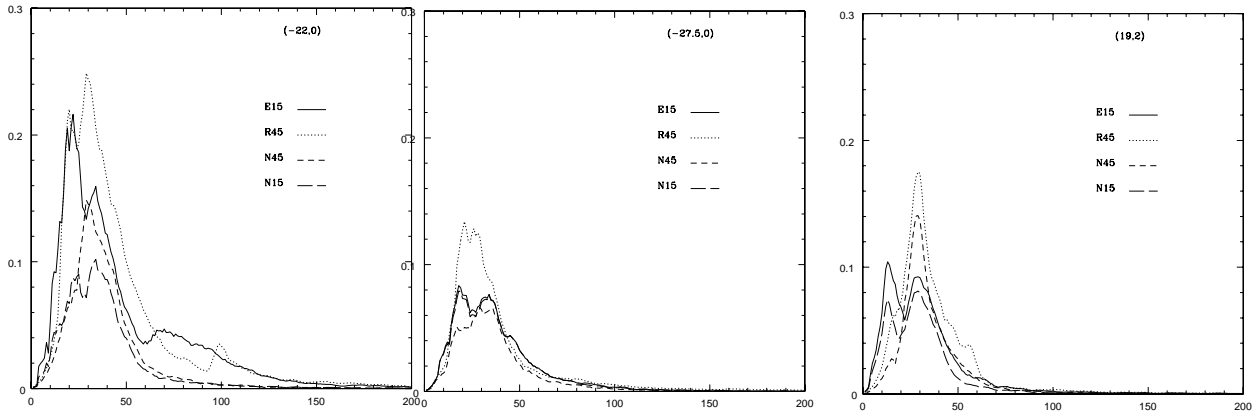


FIG. 4.— As Fig. 3a, along lines of sight toward the negative tangent point (a), a disk EROS field (b) and the high-longitude MACHO fields (c) for the models E15 and R45 and their counterparts without ring particles (N15, N45). The longitude and latitude in degrees of the lines of sight are given between brackets in the top right of each panel. The vertical scale is arbitrary, but the same for all panels (as well as Fig. 3a). The ordinate gives the event duration in days.

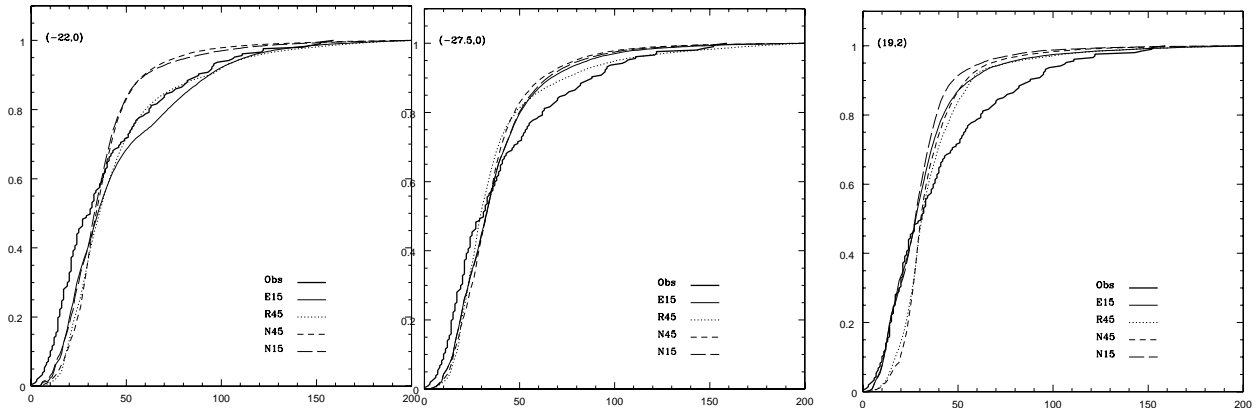


FIG. 5.— As Fig. 4, for the cumulative density distribution of event durations. The observed distribution toward Baade's window is only shown for comparison with Fig. 3b.

ring intersects the line of sight toward the galactic Centre (with  $V_{\odot}=210 \text{ km s}^{-1}$ ,  $U_{\odot}=0 \text{ km s}^{-1}$ ).

The fractional width of the inner ring in the minor-axis H-band profile of eg. NGC 3081 is about 0.2 and data on other galaxies suggest that this is a fairly standard value. Hence, we derive that the velocity dispersion in the galactic ring would be  $<0.25 \cdot 200 \text{ km s}^{-1} = 50 \text{ km s}^{-1}$ . In the following text, we will mention the influence of such a velocity dispersion in the several cases that will be discussed. However, since we are mainly interested in the influence of the geometry of the ring – ie. the streaming velocity – the standard models are without velocity dispersion. This in fact turns out to yield perfectly acceptable approximations.

The total number of particles in the ring is taken to be 10% of the number in the N-body model,  $\delta_r = 600 \text{ pc}$  and  $h_z = 380 \text{ pc}$ . (This scaleheight equals that of the N-body model (see Fux 1999) and maximizes equation (3) for  $R=2.6 \text{ kpc}$ ). A range of  $a, \phi, q$  are used (Table 1). The “Nxx” runs have no ring, only  $\phi_{\text{bar}} = \text{xx}$ .

## 5.2. Results and comparison to available data

The event-duration distribution (EDD) in the direction of the Bulge (all fields with  $0^\circ < \ell < 10^\circ$ ), for true micro-lensing events with a well-determined duration ( $\hat{t}$ , Alcock et al. 1997), shows a peak at 15–20 days with a fairly massive tail reaching well up to 150 days (data from the MACHO alert webpage (<http://darkstar.astro.washington.edu>), hence not complete, but the distribution is similar to that in Alcock et al. 1997). The median duration for the 202 events is 29 days (see Fig. 3). Models with a range of Bulge and Disk parameters and a range of forms of the initial-mass function (IMF) fail to reproduce the observed EDD consistently. The short-event tail may be explained by changing the lower mass cut-off and the exponent of the IMF, or simply the blending correction. The long-event tail of the observed distribution is more difficult to reproduce, but potentially very important. Even though it consists of only four events ( $\hat{t} > 100$  days) in the fully corrected sample (or 10 in the sample of Fig. 3), these do make up about one third of the total micro-lensing optical depth toward Baade’s window (Alcock et al. 1997).

From the relative proper motions and distances of our model (Section 5.1), we calculate the EDD for several lines of sight, following Han & Gould (1996). We set all masses to 1, to separate the influence on the micro-lensing optical depth of the kinematical distribution from that of the initial-mass function. This means we do not try to reproduce the observed MACHO EDD. In Fig. 3, 4&5, we show (cumulative) event-duration distributions ((C)EDD) for several models (Table 1), along several lines of sight. We discuss those in detail in the following subsections, but note that all models, with and without ring, with a viewing angle of  $15^\circ$  give bimodal distributions for  $\hat{t} < 50$  days for all lines of sight.

### 5.2.1. Toward the far tangent point

From the schematic drawing in Fig. 6 it is evident that near the far tangent point, a ring will give rise to a considerably different distribution of transverse velocities than a spiral arm. For a spiral arm, the transverse velocities will be slightly larger than for the underlying disk around

the distance of the tangent point and slightly smaller just in front of and behind it. This would not create an EDD significantly different from that of the disk. However, for a ring, the transverse velocities will be much smaller than in the underlying disk and, for certain viewing angles, very similar for a large range of distances along the line of sight.

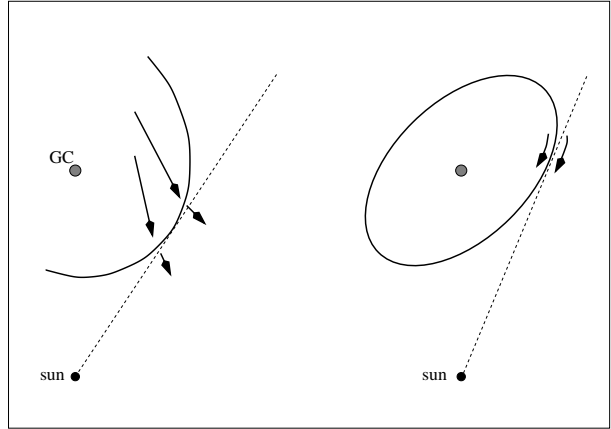


FIG. 6.— For a ring, the average stellar velocities will be along the line of sight at the tangent point, as opposed to the situation for a spiral arm. Therefore, the tangential velocities will be negligible for a ring, and will be coherent over a relatively large distance range. A spiral scatters stars passing through it onto more radial orbits, without necessarily making the tangential velocities more coherent. We can therefore expect that *at the tangent point*, a ring will give longer events on average than a spiral.

In the right-hand panels of Fig. 7 we show the longitudinal proper motion as a function of distance for particles along the line of sight toward the negative tangent point ( $\ell = -22^\circ$ ) for two ring models. The ring creates a larger distance spread for stars with similar proper motions, hence a higher micro-lensing optical depth for events with long durations, either via ring self-lensing or ring-bulge lensing. The effect is somewhat exaggerated in our simplistic approach without ring velocity dispersion, but the trend is unambiguous; an added velocity dispersion of  $50 \text{ km s}^{-1}$  perpendicular to the line of sight gives a scatter in proper motions of only  $2 \text{ mas/yr}$  at a distance of  $5 \text{ kpc}$ . In Fig. 7, we can see that this would not change the configuration significantly.

Looking at the actual EDD for this line of sight (Fig. 4&5a), we see that the events are on average longer than toward Baade’s window, even without a ring. Any observed tangent-point EDD would have to be compared to an EDD along a “clean” disk-only line of sight, not to the EDD measured toward Baade’s window. So, compared to the “no ring” EDDs in Fig. 4a, both ring models show significant excesses of long events. In fact, R45 yields longer events than E15, but for a narrower range of durations. Self-lensing gives rise to an excess of 60–100 day events for E15, whereas the extra 90–110 day events in R45 seem to come from ring-bulge events (Fig. 7). When giving the ring particles an isotropic velocity dispersion of  $50 \text{ km s}^{-1}$ , the median timeduration does not change for any of the models considered. The 95-% timeduration changes marginally; for the “Exx” models it increases by about 1 sigma ( $\sim 3$  days), for the “Rxx” models it stays the same to within 0.5 sigma.

TABLE 1  
PARAMETERS FOR THE RUNS.

Name	$\phi$	a	q
	$^{\circ}$	kpc	
<b>E15,30</b>	15,30	5	0.6
<b>R15,30</b>	15,30	4	0.8
<b>E45,75</b>	45,75	5	0.6
<b>R45,75</b>	45,75	4	0.8

NOTE.— For all runs,  
 $\phi_{\text{bar}} \equiv \phi_{\text{ring}}$  (Section 5.1).

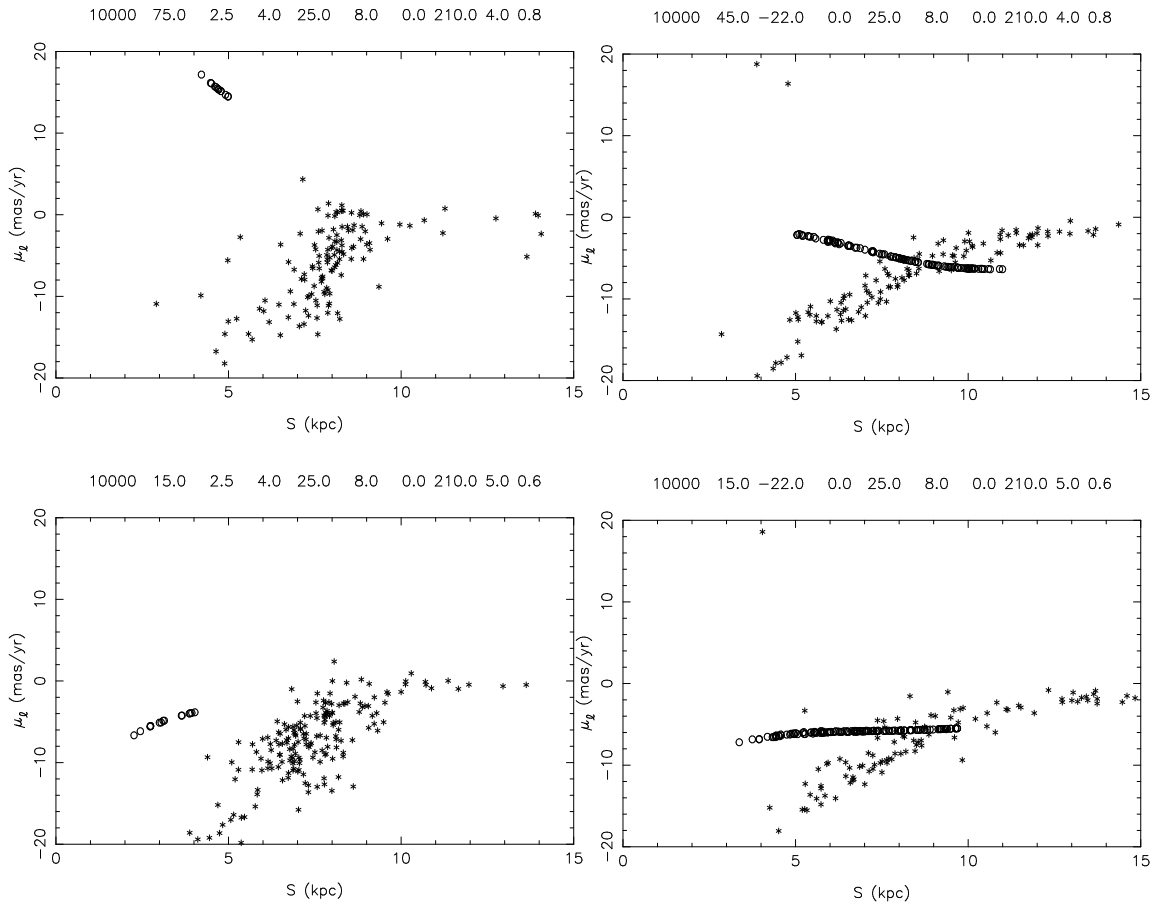


FIG. 7.— The ‘observed’ longitudinal proper motion as a function of distance from the Sun is shown for several models. The top panels are for R75 (left (a)) and R45 (right (b)), the bottom ones for E15 (c,d). All particles are within 0.1 kpc from the line of sight toward Baade’s window  $(\ell, b) = (2^{\circ}5, 4^{\circ})$  in the left panels and the negative tangent point  $(\ell, b) = (-22^{\circ}, 0^{\circ})$  in the right panels. Asterisks denote particles from the disk+bar N-body simulation (Fux 1997), circles the particles drawn from the respective analytic ring densities (see Section 5.1,  $\phi_{\text{bar}} \equiv \phi_{\text{ring}}$ ). No velocity dispersion is attributed to the ring particles; this exaggerates the effect seen in the right-hand panels slightly, but note that a velocity component of  $10 \text{ km s}^{-1}$  at a distance of 5 kpc only amounts to a proper motion of 0.4 mas/yr. The total number of ring particles is 10% of the number of N-body particles. The velocity of the local standard of rest is taken to be  $210 \text{ km s}^{-1}$ .

### 5.2.2. Toward higher longitudes

Along a line of sight beyond the tangent point (Fig. 4&5b), the ring in E15 has no effect on the EDD anymore, while R45 still gives rise to longer events (>50 days) than the others. In this direction, the EROS team (see Perdereau 1999) detected two events, of 72 and 98 days, respectively.

Fields at high positive longitudes were monitored in the MACHO experiment. Five events were observed at ( $18^\circ 77', -2^\circ$ ), with durations of 38, 88, 111, 210 and 242 days, respectively (MACHO alert webpage, field 301). In Fig. 4&5c we see that for  $\phi=15^\circ$ , both with and without ring, there is an excess of short events in this direction. For both models with ring, E15 and R45, there is a long-event tail and R45 has a significant excess of events between 40–60 days.

### 5.2.3. Toward Baade's window

Along the line of sight to the galactic Centre, a spiral arm will lower the average transverse velocities slightly, via the same deflection as shown in Fig. 6. With the bulk of the background sources at low transverse velocities, this would give rise to longer events, possibly one step closer towards accounting for the high-event-duration tail that is observed and not fully explained by disk-bulge models (Alcock et al. 1997). However, spiral-arm events do not have large micro-lensing optical depth (see Section 4).

Ring particles do contribute significantly to the micro-lensing optical depth. They can have transverse velocities either higher or lower than those of the underlying disk, depending primarily on viewing angle. For model E15, the transverse velocity of ring particles at  $\ell=0^\circ$  is  $133 \text{ km s}^{-1}$ , much lower than the local circular velocity ( $\sim 170 \text{ km s}^{-1}$ ). Hence, E15 should give ring-bulge events that are somewhat longer than disk-bulge events. Indeed, Fig. 3 shows that E15 gives more events longer than  $\sim 50$  days than N15. For higher viewing angles, the transverse velocity at  $\ell = 0^\circ$  of the ring can be very large and give rise to short events, as for R75 (Fig. 3). This can also be seen in the left panels of Fig. 7, that show the transverse proper motions as a function of distance toward Baade's window, for E15 and R75. For E15, the ring particles have the same transverse proper motions as the background distribution.

The EDD for R45 gives a similar long-event tail (>65 days) to model N15. Apparently, the addition of a ring to a bar+disk model has an effect similar to lowering the viewing angle, not only on the total micro-lensing optical depth but also on the long-event tail of the EDD. Indeed, for a viewing angle of  $45^\circ$ , the elongation does not have much influence on the proper motions of the ring particles along Baade's window line of sight and the EDD, whereas for  $15^\circ$  the rounder ring (R15) gives rise to short events like R75.

Again, with an isotropic velocity dispersion of 50

$\text{km s}^{-1}$  added to the ring-particle velocities, the median time durations remain the same, within the error of 0.2 day. The 95-% time durations remain the same for the "Rxx" models (with positive observed ring proper motions), with slightly increased scatter (1.5 days). For the "Exx" models, they decrease somewhat, with decreasing scatter. For eg. E15, the zero-dispersion 95-% time duration is  $91 \pm 3.7$  and the  $50\text{-km s}^{-1}$  95-% time duration is  $90 \pm 3.4$ . In short, the streaming velocity is by far the dominant factor in determining time durations, since the dispersion in the proper motions of the foreground particles (ring) is negligible compared to that of the background particles (bulge).

## 6. CONCLUSIONS

We present the first stellar-kinematical evidence that material in the 3-kpc arm follows closed orbits. This provides another good reason to assume that there is an inner ring in the Galaxy, such as commonly observed in other barred galaxies. As this ring crosses the line of sight towards Baade's window between the observer and the bulge region, it would be an ideal candidate to explain the high observed values for the micro-lensing optical depth  $\tau$ . Based on (infra-) red photometry of rings in external barred galaxies, we find that a ring could increase the micro-lensing optical depth to give values for  $\tau_{-1}$  within  $1.5\sigma$ , and for  $\tau_0$  very close to, (recent) observations. The exact contribution depends on the ring's semi-major axis and viewing angle and the scaleheight of the disk.

We calculate event-duration distributions for simple models with a range of viewing angles and along several lines of sight. For low viewing angles ( $<45^\circ$ ), a ringed model could yield more long events toward Baade's window than a bar+disk model, and vice versa.

We show that if the event durations toward the tangent point prove to be significantly longer than those of general disk-disk events, this is conclusive evidence in favour of the ring-, as opposed to density-wave-, hypothesis. A properly sampled EDD toward the negative-longitude tangent point, compared to a disk-only EDD, would moreover be essential to determine the values of the ring-density parameters, such as viewing angle and elongation. Since those parameters are closely connected to the parameters of the barred potential, this would provide an independent way to determine these.

Intermediate-viewing-angle ringed models show equal promise for explaining the high values of observed micro-lensing optical depth and event-duration distribution to, and are more realistic than, low-viewing-angle bar+disk-only models.

We thank Tim Axelrod for helpful discussions and Roger Fux for providing us with the full particle positions of his N-body simulation m08t3200.

## REFERENCES

- Alard, C., & Guilbert, J. 1997, A&A, 326, 1  
 Alcock, C., Allsman, R., Alves, D., Axelrod, T., Bennett, D., et al. 1997, ApJ, 479, 119  
 Alcock, C., Allsman, R., Alves, D., Axelrod, T., Becker, A., et al. 2000a, ApJ, 541, 734  
 Alcock, C., Allsman, R., Alves, D., Axelrod, T., Becker, A., et al. 2000b, ApJ, 542, 281  
 Binney, J.J., Gerhard, O.E., & Spergel, D.N. 1997, MNRAS, 288, 365  
 Bissantz, N., Englmaier, P., Binney, J., & Gerhard, O. 1997, MNRAS, 289, 651  
 Blommaert, J., van Langevelde, H., & Michiels, W. 1994, A&A, 287, 479  
 Buta, R. 1991, ApJ, 370, 130



- Buta, R., & Combes, F. 1996, *Fund. Cosmic Physics*, Vol.17, p.95
- Buta, R., Alpert, A., Cobb, M., Crocker, D., & Purcell, G. 1998, *AJ*, 116, 1142
- Buta, R., & Purcell, G. 1998, *AJ*, 115, 484
- Cohen, R., Cong, H., Dame, M., & Thaddeus, P. 1980, *ApJ*, 239, L53
- Englmaier, P., & Gerhard, O. 1999, *MNRAS*, 304, 512
- Fuchs, B., Jahreiss, H., & Flynn, C. 1998, *A&A*, 339, 405
- Fux, R. 1997, *A&A*, 327, 983
- Gould, A., Flynn, C., & Bahcall, J. 1998, *ApJ*, 503, 798
- Hammersley, P., Garzon, F., Mahoney, T., & Calbet, X. 1994, *MNRAS*, 269, 753
- Han, C., & Gould, A. 1996, *ApJ*, 467, 540
- Kalnajs, A.J. 1991, In: Sundelius (ed.), *Dynamics of disc Galaxies*, Göteborg, p. 323
- Kalnajs, A.J. 1996, In: Sandqvist, Lindblad (eds.), *Barred Galaxies and Circumnuclear Activity*, Nobel Symp. 98, Springer, Heidelberg, p. 165
- Kiraga, M., & Paczynski, B. 1994, *ApJ*, 430, L101
- Kroupa, P. 1998, In: Rebolo, Eduardo, Zapatero (eds.), *Brown dwarfs and extrasolar planets*, PASPC 134, p.483
- Kuijken, K., & Gilmore, G. 1989, *MNRAS*, 239, 651
- Lépine, J., Ortiz, R., & Epchtein, N. 1995, *A&A*, 299, 453
- Minniti, D. 1996, *ApJ*, 459, 175
- Nikolaev, S., & Weinberg, M. 1997, *ApJ*, 487, 885
- Oort, J.H. 1977, *ARA&A*, 15, 295
- Perdereau, O. 1999, In: Gibson, B., Axelrod, T., Putman, M. (eds.) *The Third Stromlo Symposium: The Galactic Halo*, PASPC 165, San Francisco, p. 370
- Popowski, P., Cook, K., Drake, A., Marshall, S., Nelson, C., et al. 2000 AAS 197 #04.17 (also astro-ph 0005466)
- Sevenster, M.N. 1999, *MNRAS*, 310, 629
- Sevenster, M., Saha, P., Valls-Gabaud, D., & Fux, R. 1999, *MNRAS*, 307, 584
- Shane, W. 1972, *A&A*, 16, 118
- Taylor, J.H., & Cordes, J.M. 1993, *ApJ*, 411, 674
- Udalski, A., Szymanski, M., Stanek, K., Kaluzny, J., Kubiak, M., et al. 1994, *AcA*, 44, 165
- Wielen, R. 1977, *A&A*, 60, 263
- Yuan, C. 1984, *ApJ*, 281, 600
- Zhao, H.S., & Mao, S. 1996, *MNRAS*, 283, 1197
- Zhao, H.S., Rich, R.M., & Spergel, D.N. 1996, *MNRAS*, 282, 175